Macrophage Il-1beta protects against mycobacterial infection downstream of Hif-1alpha in zebrafish.

[1,2]Nikolay V. Ogryzko, [1,3]Amy Lewis, [3]Heather L. Wilson, [4]Annemarie H. Meijer, [1,3]Stephen A. Renshaw and [1,3,]*Philip M. Elks

[1]The Bateson Centre, University of Sheffield, Western Bank, Sheffield, UK.

[2]MRC Centre for Inflammation Research, University of Edinburgh, Little France Crescent, Edinburgh, UK.

[3]Department of Infection and Immunity and Cardiovascular Disease, University of Sheffield, Western Bank, Sheffield, UK.

[4]Institute of Biology, Leiden University, Leiden, The Netherlands.

*Corresponding author:

Email: p.elks@sheffield.ac.uk (PME)

Abstract

Drug resistant mycobacteria are a rising problem worldwide. There is an urgent need to understand the immune response to TB to identify host targets that, if targeted therapeutically, could be used to tackle these currently untreatable infections. Here, we use an Il-1β fluorescent transgenic line to show that there is an early innate immune pro-inflammatory response to well-established zebrafish models of inflammation and *Mycobacterium marinum* (Mm) infection. We demonstrate that host-derived hypoxia signalling, mediated by the Hif-1α transcription factor, can prime macrophages with increased levels of Il-1β in the absence of infection. Moreover, Il-1β upregulates neutrophil antimicrobial nitric oxide production and is protective against infection. Our data link Hif-1α to proinflammatory macrophage Il-1β transcription during early mycobacterial infection and highlight how host-derived Hif-1α may be a promising drug target to stimulate the innate immune response to better deal with infection.

Introduction

Pulmonary tuberculosis (TB) is a major world health problem caused by the bacillus *Mycobacterium tuberculosis* (*Mtb*) (1). It is a current priority for infectious disease research due to increasing rates of multi- and totally- drug resistant strains causing high levels of mortality, especially in the immunocompromised (2). Mycobacteria are specialised at evading killing mechanisms of the immune system to survive. Mycobacteria and immune cells create a highly organised niche, called the granuloma, in which Mtb can proliferate or enter a latent phase, protected from the immune system (3, 4). In human Mtb infection, bacteria first encounter cells of the innate immune system in and around the lungs, either macrophages in the

alveolar space or neutrophils in the surrounding capillary vasculature, before the involvement of adaptive immunity and granuloma formation (5, 6). These initial phagocytosis events are followed by the attraction of other innate immune cells which signal to draining lymph nodes to activate the adaptive immune response, signs of which only become apparent 3 to 8 weeks after infection in humans (6). Although granuloma formation is reasonably well characterised, the initial interactions of the bacteria with the host innate immune cells are less well defined.

Mtb, like many other bacterial and pathogenic microbes, triggers a pro-inflammatory immune response via the activation of TLRs (Toll-like receptors) (7). The activation of the innate immune cells via TLR signalling is a critical early host response to many invading pathogens for successful clearance of infection and, in the absence of TLR signalling, mycobacteria grow unchecked to cause systemic infection (8). Although mycobacteria can hijack host leukocytes to create a niche for their growth, in zebrafish models many of the initial Mm inoculum are neutralised by macrophages and neutrophils before infection can take hold (9, 10). Early mycobacterial interaction with host leukocytes is critical for the pathogen, and manipulation of the macrophage by the bacteria is required for establishment of a permissive niche in which the bacteria can grow and build its host derived protective structure, the granuloma (11, 12). Greater understanding of the diverse phenotype of macrophages immediately after infection may allow therapeutic tuning to provide maximal early control of mycobacteria during infection (13, 14). Recent studies in optically translucent zebrafish infection models have indicated that initial interactions between Mm and macrophages and neutrophils are more complex than originally thought, with successive rounds of bacterial internalisation and leukocyte cell death leading to

granuloma formation (9, 15, 16). The immune molecular mechanisms involved in these early processes are poorly understood.

We have previously demonstrated in a zebrafish/Mm model of TB that the initial immune response to infection can be enhanced by stabilising host-derived Hif-1α (hypoxia inducible factor -1 alpha), leading to reduced bacterial burden (17). Hif-1α is a major transcriptional regulator of the cellular response to hypoxia, that has been implicated in the activation of macrophages and neutrophils during infection and inflammatory processes (18, 19). Stabilisation of Hif-1α in zebrafish upregulated pro-inflammatory neutrophil nitric oxide (NO) production leading to lower mycobacterial burden (17, 20). The mechanisms by which pro-inflammatory cytokines associated with this NO increase are regulated by Hif-1α signalling is not known.

IL-1β is a critical macrophage-derived activator of immune cells with wide-ranging and complex effects on immune signalling and downstream pathways. IL-1β has been shown to be upregulated in the onset and formation of Mm and Mtb granulomas (21–23). We hypothesised that IL-1β would be activated in specific immune cell populations early in Mm infection, (within 1-day post-infection, pre-granuloma formation) and that Hif-1α acts via altered expression of this important pro-inflammatory mediator to confer protection against mycobacterial infection. Here, using the zebrafish Mm model and fluorescent transgenic lines, we show that that *il-1β* is transcriptionally upregulated in macrophages early during *in vivo* infection. Stabilisation of Hif-1α upregulates *il-1β* transcription in macrophages in the absence of infection. *il-1β* signalling is required for protective NO production by neutrophils and a subsequent decrease in infection. Our data indicate that protective Hif-1α mediated NO is at least partially regulated by the key pro-inflammatory mediator Il-

1β, increasing our understanding of the mechanism of action of the potential therapeutic target, Hif-1α, as a host-derived factor in TB.

Materials and Methods

Zebrafish and bacterial strains

Zebrafish were raised and maintained on a 14:10-hour light/dark cycle at 28 degrees C, according to standard protocols (24), in UK Home Office approved facilities at The Bateson Centre aquaria at the University of Sheffield. Strains used were Nacre (wildtype), *Tg(mpeg1:mCherry-F)ump2Tg, TgBAC(il-1β:eGFP)sh445 Tg(mpeg1:mCherryCAAX)sh378* and *Tg(lyz:Ds- RED2)nz50* (25–28).

Mm infection experiments were performed using M. marinum M (ATCC #BAA-535), containing a psMT3-mCherry or psMT3 mCrimson vector (29). Injection inoculum was prepared from an overnight liquid culture in the log-phase of growth resuspended in 2% polyvinylpyrrolidone40 (PVP40) solution (CalBiochem) as previously described (30). 100-150 colony forming units (CFU) were injected into the caudal vein at 28-30hpf as previously described (31).

Generation of *TgBAC(il-1α:GFP)sh445* transgenic and *il-1β*^{SH446}/ *il-1β*^{SH446} mutant zebrafish

An eGFP SV40 polyadenylation cassette inserted at the *il-1β* ATG start site of zebrafish BAC CH-211-147h23 using established protocols (32). Inverted Tol2 elements were inserted into the chloramphenicol coding sequence and the resulting modified BAC was used to generate *TgBAC(il-1β:eGFP)sh445*.

il-1-/- (*il-1β*^{SH446}/ *il-1β*^{SH446}) mutant embryos were generated by CRISPR-Cas9 mediated mutagenesis targeted around an Mwo1 restriction site in the third exon of *il-1β* using the method described by Hruscha et al (2013) and the template sequence 5'-AAAGCACCGACTCGGTGCCACTTTTTCAAGTTGATAACGGACTAGCCTTATTTTAACTTGCTATTTCTAGCTCTAAAAC**TGAGCATGTCCAGCACCTC**GGCTATAGTGAGT CGTATTACGC-3' (*il-1β* target sequence in bold). PCR with il-1gF 5'-TAAGGAAAAACTCACTTC-3' and il-1gR 5'ATACGTGGACATGCTGAA3' and subsequent Mwo1 digestion were used for genotyping.

Morpholino knockdown of *il-1β*

The *il-1bβ* morpholino (Genetools) was used as previously reported (33). A standard control morpholino (Genetools) was used as a negative control.

Confocal microscopy of transgenic larvae

1dpi and 4dpi transgenic zebrafish larvae infected with fluorescent Mm strains were mounted in 0.8-1% low melting point agarose (Sigma-Aldrich) and imaged on a Leica TCS-SPE confocal on an inverted Leica DMi8 base and imaged using 20x or 40x objective lenses.

For quantification purposes acquisition settings and area of imaging (in the caudal vein region) were kept the same across groups. Corrected total cell fluorescence was calculated for each immune-stained cell using Image J as previously described (17, 20).

Tailfin transection

Inflammation was induced in zebrafish embryos by tail transection at 2 or 3dpf as described previously (34). Embryos were anesthetised by immersion in 0.168 mg/mL Tricaine (Sigma-Aldrich), and tail transection was performed using a microscalpel (World Precision Instruments).

qPCR of *il-1β*

qPCR was performed on 1dpi Mm infected (or PVP control) embryos as previously described (35). The following primers were used: *il-1β*, accession number NM_212844, forward primer: GAACAGAATGAAGCACATCAAACC, reverse primer: ACGGCACTGAATCCACCAC, *ppial* control, accession number AY391451, forward primer: ACACTGAAACACGGAGGCAAG, reverse primer: CATCCACAACCTTCCCGAACAC.

Bacterial pixel count

Mm mCherry infected zebrafish larvae were imaged at 4dpi on an inverted Leica DMi8 with a 2.5x objective lens. Brightfield and fluorescent images were captured using a Hammamatsu OrcaV4 camera. Bacterial burden was assessed using dedicated pixel counting software as previously described (36).

RNA injections

Embryos were injected with dominant *hif-1αb* variant RNA at the one cell stage as previously described (19). *hif-1α* variants used were dominant active (DA) and dominant negative (DN) *hif-1α* (ZFIN: *hif1ab*). Phenol red (PR) (Sigma Aldrich) was used as a vehicle control.

Anti-nitrotyrosine antibody staining

Larvae were fixed in 4% paraformaldehyde in PBS overnight at 4°C and nitrotyrosine levels were immune-labelled using a rabbit polyclonal anti-nitrotyrosine antibody (Merck Millipore 06-284) and were detected using an Alexa Fluor conjugated secondary antibody (Invitrogen Life Technologies) as previously described (17, 20).

Statistical analysis

All data were analysed (Prism 7.0, GraphPad Software) using unpaired, two-tailed t-tests for comparisons between two groups and one-way ANOVA (with Bonferonni post-test adjustment) for other data. P values shown are: $*P < .05$, $**P < .01$, and $***P < .001$.

Results

Hif-1α mediated nitrotyrosine production is Myd-88 independent.

We have previously shown that stabilisation of Hif-1α induces pro-inflammatory neutrophil nitric oxide production, via inducible nitric oxide (iNOS) (17, 20). First, we aimed to determine whether Hif-1α induced increase in nitrotyrosine is dependent on TLR signalling, having previously demonstrated that Mm activation of nitrotyrosine is TLR mediated (20). We therefore knocked down TLR signalling by targeting a critical adapter of TLR signalling, *myd88*, using a well-characterised and validated morpholino (an antisense oligonucleotide that blocks translation) (37). The *myd88* morpholino was unable to block the DA Hif-1α mediated nitrotyrosine signal (Figure 1A and B). These data indicate that DA Hif-1α mediated pro-inflammatory signalling is independent of TLR signalling and therefore likely to be separate from bacterial

sensing mechanisms. We hypothesised that this increase in NO may be a part of an increased pro-inflammatory profile in innate immune cells.

Inflammation induces GFP expression in a *TgBAC(il-1β:GFP)SH445* transgenic line

Il-1β is a major macrophage-derived pro-inflammatory cytokine that is upregulated in both inflammation and infection. We have previously shown upregulation of *il-1β* message after induction of inflammation by qPCR and wholemount *in situ* hybridisation (WISH) in the zebrafish (38). We hypothesised that Il-1β is a major pro-inflammatory cytokine that would be upregulated by both mycobacterial infection and Hif-1α stabilisation. To investigate *il-1β* expression *in vivo*, we developed a BAC (bacterial artificial chromosome) derived *il-1β* promoter driven GFP line, *TgBAC(il-1β:GFP)SH445*, to assess *il-1β* expression in real-time during mycobacterial infection. We sought to examine *il-1β:GFP* expression in our well-established inflammation assay before investigating its expression during mycobacterial infection. *il-1β:GFP* recapitulates *il-1β* mRNA expression in response to tail transection (Figure 2A and B) (38), although, as expected, the synthesis of GFP occurs over a longer timescale than that of *il-1β* mRNA detected by WISH. Neutrophils are the first cells to respond to tailfin transection with increased *il-1β:GFP*, with fluorescence first observed at 1hpw (hours post-wounding) and still present at 6hpw (Figure 2C and D). Macrophages are slower to respond, with no *il-1β:GFP* expression observed at 1hpw, with expression present at 6hpw (Figure 2E). Having demonstrated that the il-1β:GFP is responsive to inflammation in similar cells

over a similar timespan as the *in situ* hybridisation, we sought to investigate its regulation during mycobacterial infection.

il-1β:GFP is upregulated in macrophages at early and later stage Mm infection

The initial phase of Mm infection in zebrafish is characterised by a short period of greatly increased pro-inflammatory signalling (before 1 day post-infection, dpi) where the immune system reacts to Mm infection. This is followed by a lag-phase of decreased activity which allows for granuloma formation between 2-3dpi, before cytokine levels rise again in formed larval granulomas at 4dpi (9, 39). However, the levels of pro-inflammatory cytokines have only been previously studied at a transcriptional level in whole embryos or FACS sorted cells, rather than detecting levels *in situ*, over time, in an intact organism (39).

il-1β is one of the most readily detectable pro-inflammatory cytokines during early stages of Mm infection, upregulated 1.7 fold at 1dpi by wholebody qPCR, compared to PVP injection controls (Figure 3A). We used the *TgBAC(il-1β:GFP)sh445* line to show that GFP is expressed in cells proximal to Mm infection sites at pre-granuloma phases (1dpi) and in larval granulomas (4dpi) (Figure 3B). The earliest timepoint at which faint *il-1β:GFP* could be detected by confocal microscopy was between 6 and 8 hours post infection, consistent with rapid transcriptional activation of the *il-1β* promoter after infection (Figure 3C) and similar to the timing of macrophage *il-1β:GFP* expression after tailfin transection (Figure 2D). *il-1β:GFP* was predominantly upregulated in infected macrophages at 1dpi (Figure 3D) and these macrophages were activated in appearance, with highly dynamic cellular processes (Supplemental Movie 1). These data demonstrate that during early stages of infection *il-1β* is

transcriptionally activated in infected macrophages as part of an early pro-inflammatory response.

Stabilisation of Hif-1α upregulates *il-1β:GFP* at early stages of infection

We have previously shown that stabilisation of Hif-1α induces neutrophil pro-inflammatory nitric oxide production (17, 20). We hypothesised that this may be a part of an increased pro-inflammatory profile in innate immune cells, therefore we tested whether Hif-1α is upregulating a pro-inflammatory program in the absence of infection using the *il-1β:GFP* transgenic line. Dominant active Hif-1α significantly increased *il-1β:GFP* expression in the absence of Mm infection at 2dpf, while dominant negative Hif-1α caused no difference in *il-1β:GFP* expression (Figure 4A and B). These data indicate that *il-1β* expression is part of a pro-inflammatory response to increased Hif-1α levels, a response that could aid the host response to Mm challenge.

Inhibition of *il-1β* increases Mm burden and inhibits the Hif-1α nitric oxide response

Il-1β is a major pro-inflammatory cytokine that in many infections is instrumental in coordinating the immune response (40, 41). We sought to test whether Il-1β was important in early Mm infection. When Il-1β was blocked using a well-characterised and validated *il-1β* morpholino, the morphants showed significantly increased infection compared to a control morphants (Figure 5A). DA Hif-1α was not sufficient to reduce Mm infection levels when *il-1β* expression was blocked (Figure 5A) suggesting that the *il-1β* response to Mm infection is critical to control infection.

These results were supported by generation of an *il-1β* null mutant (*il-1β*^{SH446}/ *il-1β*^{SH446}), in which DA Hif-1α also did not decrease infection, while in wildtype siblings infection was reduced (Figure S1 and Figure 5B).

We have previously demonstrated that inhibiting production of nitric oxide by Nos2 can block the antimicrobial effect of DA Hif-1α (17). Blocking Il-1β production also significantly dampened the neutrophil nitric oxide response after Mm infection at 1dpi (Figure 5C-E). Furthermore, Il-1β MO blocked the increased production of nitrotyrosine by DA Hif-1α (Figure 5C-E). These results show that Hif-1α activation of Nos2 may, at least in part, be acting through *il-1β* activation and hint at a much more complex regulation of pro-inflammatory signalling by Hif-1α than simply acting on Hif responsive elements (HREs) in the promoter of Nos2.

Discussion

Antimicrobial resistance is a rising problem in TB infections worldwide and there is an urgent need to understand the regulation of host-immunity by TB so that we can target host-derived factors to help tackle disease. Our data identify an early pro-inflammatory response, involving macrophage *il-1β* expression, that is important for the onset of early disease. Using a well-established zebrafish Mm model of TB, we show that manipulation of Hif-1α can stimulate this pro-inflammatory network, aiding the host fight against infection. Specifically, we identify that Hif-1α driven Il-1β contributes to the NO response, a response we have previously shown to be host protective (17, 20).

Here, we took advantage of a novel transgenic zebrafish line to understand the dynamics and cell specificity of *il-1β* production in inflammation and mycobacterial infection, specifically focussing on the understudied early stages (<1dpi) of the

innate immune response to TB infection. We confirmed that the *il-1β:GFP* expression of our line was faithful to *il-1β* transcription by following its expression in a well-characterised tailfin transection model of inflammation and comparison to *in situ* hybridisation data (34, 38). Furthermore, the expression pattern of our BAC transgenic line closely matches another recently published BAC promoter driven *il-1β* transgenic (42). The *il-1β:GFP* line also displayed some GFP signal in muscle and epithelial cells in the tail. Similar GFP expression can be seen when driven by NF-kB response elements (43) but not by WISH, suggesting this might be off-target expression resulting from the promoter region missing some negative regulatory elements, however, it could also be specific expression that is at too low a level to be detectable by *in situ* hybridisation. Although previous studies have shown *il-1β:GFP* to be upregulated in leukocytes at a tailfin transection (42), we combined the *il-1β:GFP* line with leukocyte specific transgenics to show that neutrophils are the first to respond at the wound, with macrophages both migrating to and upregulating *il-1β:GFP* at later timepoints.

The Mtb granuloma is widely studied, both in terms of immunohistochemistry of human granulomas, and in mammalian models (44–46). These studies have demonstrated that the granuloma is rich in pro-inflammatory cytokine production. This pro-inflammatory environment has been observed in human TB, with IL-1β found to be in high levels in pleural fluid from TB patients with granulomas present (47). Here we observe that the pro-inflammatory response is present at pre-granuloma stages. Lack of a pro-inflammatory response has been linked to poor treatment outcomes indicating that this host response is important even in the presence of antimycobacterial agents (48). The upregulation of proinflammatory cytokines in mycobacterial infection has also been shown in the zebrafish/Mm larval

model of TB granulomas, but previous studies have mainly relied on immunohistochemistry and/or transcriptomics data from either wholebody larvae or FACs sorted immune cell populations (25, 39). Using live cell imaging we found that *il-1β* transcription was upregulated at the granuloma formation stage, however we also demonstrated that it is upregulated before the granuloma stage within 6-8 hours hpi. Upon infection *il-1β:GFP* expression was predominantly upregulated in infected macrophages indicating that within the first 24 hours of infection there is a macrophage pro-inflammatory response. Murine and human cell studies have indicated that macrophages are able to produce IL-1β a few hours after mycobacterial challenge indicating that an early response is also present in mammalian systems, at least on a cellular level (21, 49). Our observations are in line with our previous observation of Hif-1α signalling early after infection (detected using a *phd3:GFP* transgenic line), which was also observed in infected macrophages at 1dpi (17), indicating that *il-1β*, alongside Hif signalling, is part of an immediate pro-inflammatory macrophage response.

We have previously demonstrated that stabilisation of Hif-1α can aid the zebrafish host control Mm infection, at least in part by priming neutrophils with increased nitrotyrosine generated by the Nos2 enzyme (17). This increase in neutrophil NO is independent of bacteria and here we demonstrate that it is independent of TLR signalling, indicating that this process is independent of bacterial sensing mechanisms. We also show that stabilisation of Hif-1α upregulates pro-inflammatory macrophage *il-1β* expression in the absence of an infection challenge. If Il-1β activity is repressed then Hif-1α induced reduction in bacterial burden is abrogated, alongside the Hif-1α dependent increase in NO production. These data show regulation of both Nos2 and Il-1β by Hif-1α, and that Hif-1α driven NO production is

partially dependent on Il-1β induction. Both human NOS-2 and IL-1β have HREs (HIF responsive elements) in their promoters and direct regulation by HIF-α signalling has been previously demonstrated *in vitro* (50, 51). Our data do not rule out direct regulation of Nos2 by Hif-1α, as blocking Il-1β is likely to have wider spread immune effects, however they do suggest that Nos2 is partially upregulated by Il-1β in the stabilised Hif-1α context. These observations, alongside our finding that blocking Il-1β, primarily observed in macrophages, can block Hif-1α induced neutrophil nitrotyrosine production, indicate a close interplay between macrophages and neutrophils during early infection that is not yet fully understood.

IL-1β is an important pro-inflammatory cytokine, but its processing by caspases also plays a crucial role in immune cell pyroptosis mediated by the inflammasome (52). Recent findings in the Mm/zebrafish model indicate that neutrophils and macrophages can efficiently phagocytose bacteria and undergo rounds of cell death and re-uptake during the initial days of infection (9). Although here we show a role for early pro-inflammatory *il-1β* transcription during Mm infection, the role of Il-1β processing and inflammasome induced pyroptosis/cell death in these early Mm immune processes remain undetermined.

In conclusion, our data demonstrate an early pro-inflammatory response of Mm infected macrophages. By stabilising Hif-1α, macrophage Il-1β can be primed in the absence of infection and is protective upon Mm infection via neutrophil nitric oxide production. Therapeutic strategies targeting these signalling mechanisms could decrease the level of initial mycobacteria in patients and act to block the development of active TB by reactivation of macrophage pro-inflammatory stimuli. Therapies that target host-derived signalling pathways such as these would be

beneficial against multidrug resistant strains and could act to shorten the currently long antibiotic therapies required to clear TB from patients.

Acknowledgements

The authors would like to thank the Bateson Centre Aquarium Team at the University of Sheffield for fish care. We gratefully thank Georges Lutfalla (Montpellier University) for providing the *Tg(mpeg1:mCherry-F)ump2Tg line,* Lalita Ramakrishnan (University of Washington, Seattle) for M. marinum strains and Astrid van der Sar (VU University Medical Center, Amsterdam) for the pSMT3-mCherry vector.

P.M.E. is funded by a Sir Henry Dale Fellowship jointly funded by the Wellcome Trust and the Royal Society (Grant Number 105570/Z/14/Z). S.A.R. is funded by an MRC Programme Grant (MR/M004864/1). A.H.M. is funded by a Smart Mix Program of the Netherlands Ministry of Economic Affairs and the Ministry of Education, Culture and Science. NVO and HLW are funded by British Heart Foundation (BHF) project grant (PG/13/80/30443) and Biotechnology and Biological Sciences Research Council (BBSRC) project grant (BB/L000830/1).

Author Contributions

Conceived and designed the experiments: PME, SAR, NVO. Performed the experiments: PME, NVO, AL. Analysed the data: PME, NVO, HW, AHM, SAR. Wrote the paper: PME, NVO, SAR.

1. World Health Organization. 2016. Multidrug-Resistant Tuberculosis (MDR-TB).

393 Burden, Glob Treat Enroll O N Mdr-tb Outcomes, Treat 2015–2016.

394 2. Koul A, Arnoult E, Lounis N, Guillemont J, Andries K. 2011. The challenge of new drug
395 discovery for tuberculosis. Nature 469:483–490.

396 3. Podinovskaia M, Lee W, Caldwell S, Russell DG. 2013. Infection of macrophages with
397 Mycobacterium tuberculosis induces global modifications to phagosomal function.
398 Cell Microbiol 15:843–859.

399 4. Ramakrishnan L. 2012. Revisiting the role of the granuloma in tuberculosis. Nat Rev
400 Immunol.

401 5. Lerner TR, Borel S, Gutierrez MG. 2015. The innate immune response in human
402 tuberculosis. Cell Microbiol.

403 6. Jasenosky LD, Scriba TJ, Hanekom WA, Goldfeld AE. 2015. T cells and adaptive
404 immunity to Mycobacterium tuberculosis in humans. Immunol Rev 264:74–87.

405 7. Mortaz E, Adcock IM, Tabarsi P, Masjedi MR, Mansouri D, Velayati AA, Casanova JL,
406 Barnes PJ. 2015. Interaction of Pattern Recognition Receptors with Mycobacterium
407 Tuberculosis. J Clin Immunol 35.

408 8. van der Vaart M, van Soest JJ, Spaink HP, Meijer AH. 2013. Functional analysis of a
409 zebrafish myd88 mutant identifies key transcriptional components of the innate
410 immune system. Dis Model Mech2013/03/09.

411 9. Hosseini R, Lamers GEM, Soltani HM, Meijer AH, Spaink HP, Schaaf MJM. 2016.
412 Efferocytosis and extrusion of leukocytes determine the progression of early
413 mycobacterial pathogenesis. J Cell Sci 129:3385–3395.

414 10. Cambier CJ, Takaki KK, Larson RP, Hernandez RE, Tobin DM, Urdahl KB, Cosma CL,
415 Ramakrishnan L. 2013. Mycobacteria manipulate macrophage recruitment through
416 coordinated use of membrane lipids. Nature 505:218–222.

417 11. Meijer AH. 2016. Protection and pathology in TB: learning from the zebrafish model.
418 Semin Immunopathol.
419 12. Guirado E, Schlesinger LS, Kaplan G. 2013. Macrophages in tuberculosis: Friend or foe.
420 Semin Immunopathol.
421 13. McClean CM, Tobin DM. 2016. Macrophage form, function, and phenotype in
422 mycobacterial infection: Lessons from tuberculosis and other diseases. Pathog Dis.
423 14. Dorhoi A, Kaufmann SHE. 2015. Versatile myeloid cell subsets contribute to
424 tuberculosis-associated inflammation. Eur J Immunol 45:2191–2202.
425 15. Cambier CJ, O'Leary SM, O'Sullivan MP, Keane J, Ramakrishnan L. 2017. Phenolic
426 Glycolipid Facilitates Mycobacterial Escape from Microbicidal Tissue-Resident
427 Macrophages. Immunity.
428 16. Elks PM, Renshaw SA, Meijer AH, Walmsley SR, van Eeden FJ. 2015. Exploring the
429 HIFs, buts and maybes of hypoxia signalling in disease: lessons from zebrafish models.
430 Dis Model Mech 8:1349–1360.
431 17. Elks PM, Brizee S, van der Vaart M, Walmsley SR, van Eeden FJ, Renshaw SA, Meijer
432 AH. 2013. PLOS Pathogens: Hypoxia Inducible Factor Signaling Modulates
433 Susceptibility to Mycobacterial Infection via a Nitric Oxide Dependent Mechanism.
434 PLoS Pathog 9:e1003789.
435 18. Cramer T, Yamanishi Y, Clausen BE, Forster I, Pawlinski R, Mackman N, Haase VH,
436 Jaenisch R, Corr M, Nizet V, Firestein GS, Gerber HP, Ferrara N, Johnson RS. 2003. HIF-
437 1alpha is essential for myeloid cell-mediated inflammation. Cell2003/03/12. 112:645–
438 657.
439 19. Elks PM, van Eeden FJ, Dixon G, Wang X, Reyes-Aldasoro CC, Ingham PW, Whyte MK,
440 Walmsley SR, Renshaw SA. 2011. Activation of hypoxia-inducible factor-1alpha (Hif-

441 1alpha) delays inflammation resolution by reducing neutrophil apoptosis and reverse
442 migration in a zebrafish inflammation model. Blood2011/05/11. 118:712–722.
443 20. Elks PM, Van Der Vaart M, Van Hensbergen V, Schutz E, Redd MJ, Murayama E,
444 Spaink HP, Meijer AH. 2014. Mycobacteria counteract a TLR-mediated nitrosative
445 defense mechanism in a zebrafish infection model. PLoS One 9.
446 21. Di Paolo NC, Shafiani S, Day T, Papayannoupoulou T, Russell DW, Iwakura Y, Sherman
447 D, Urdahl K, Shayakhmetov DM. 2015. Interdependence between Interleukin-1 and
448 Tumor Necrosis Factor Regulates TNF-Dependent Control of Mycobacterium
449 tuberculosis Infection. Immunity 43:1125–1136.
450 22. Bourigault M-L, Segueni N, Rose S, Court N, Vacher R, Vasseur V, Erard F, Le Bert M,
451 Garcia I, Iwakura Y, Jacobs M, Ryffel B, Quesniaux VFJ. 2013. Relative contribution of
452 IL-1α, IL-1β and TNF to the host response to Mycobacterium tuberculosis and
453 attenuated M. bovis BCG. Immunity, Inflamm Dis 1:47–62.
454 23. Novikov A, Cardone M, Thompson R, Shenderov K, Kirschman KD, Mayer-Barber KD,
455 Myers TG, Rabin RL, Trinchieri G, Sher A, Feng CG. 2011. Mycobacterium tuberculosis
456 triggers host type I IFN signaling to regulate IL-1β production in human macrophages.
457 J Immunol 187:2540–7.
458 24. Nusslein-Volhard C DR. 2002. Zebrafish: A Practical Approach1st ed. Oxford University
459 Press, Oxford.
460 25. Marjoram L, Alvers A, Deerhake ME, Bagwell J, Mankiewicz J, Cocchiaro JL, Beerman
461 RW, Willer J, Sumigray KD, Katsanis N, Tobin DM, Rawls JF, Goll MG, Bagnat M. 2015.
462 Epigenetic control of intestinal barrier function and inflammation in zebrafish. Proc
463 Natl Acad Sci U S A 112:2770–5.
464 26. Bojarczuk A, Miller KA, Hotham R, Lewis A, Ogryzko N V., Kamuyango AA, Frost H,

465 Gibson RH, Stillman E, May RC, Renshaw SA, Johnston SA. 2016. Cryptococcus
466 neoformans Intracellular Proliferation and Capsule Size Determines Early Macrophage
467 Control of Infection. Sci Rep 6:21489.
468 27. Nguyen-Chi M, Laplace-Builhe B, Travnickova J, Luz-Crawford P, Tejedor G, Phan QT,
469 Duroux-Richard I, Levraud JP, Kissa K, Lutfalla G, Jorgensen C, Djouad F. 2015.
470 Identification of polarized macrophage subsets in zebrafish. Elife 4.
471 28. Hall C, Flores M V, Storm T, Crosier K, Crosier P. 2007. The zebrafish lysozyme C
472 promoter drives myeloid-specific expression in transgenic fish. BMC Dev
473 Biol2007/05/05. 7:42.
474 29. van der Sar AM, Spaink HP, Zakrzewska A, Bitter W, Meijer AH. 2009. Specificity of the
475 zebrafish host transcriptome response to acute and chronic mycobacterial infection
476 and the role of innate and adaptive immune components. Mol Immunol2009/05/05.
477 46:2317–2332.
478 30. Cui C, Benard EL, Kanwal Z, Stockhammer OW, van der Vaart M, Zakrzewska A, Spaink
479 HP, Meijer AH. 2011. Infectious disease modeling and innate immune function in
480 zebrafish embryos. Methods Cell Biol2011/09/29. 105:273–308.
481 31. Benard EL, van der Sar AM, Ellett F, Lieschke GJ, Spaink HP, Meijer AH. 2012. Infection
482 of zebrafish embryos with intracellular bacterial pathogens. J Vis Exp2012/03/29.
483 32. Renshaw SA, Loynes CA, Trushell DM, Elworthy S, Ingham PW, Whyte MK. 2006. A
484 transgenic zebrafish model of neutrophilic inflammation. Blood2006/08/24.
485 108:3976–3978.
486 33. López-Muñoz A, Sepulcre MP, Roca FJ, Figueras A, Meseguer J, Mulero V. 2011.
487 Evolutionary conserved pro-inflammatory and antigen presentation functions of
488 zebrafish IFN?? revealed by transcriptomic and functional analysis. Mol Immunol

489 48:1073–1083.
490 34. Renshaw S, Loynes C. 2006. A transgenic zebrafish model of neutrophilic
491 inflammation. Blood… 108:3976–3978.
492 35. Van Der Vaart M, Korbee CJ, Lamers GEM, Tengeler AC, Hosseini R, Haks MC,
493 Ottenhoff THM, Spaink HP, Meijer AH. 2014. The DNA damage-regulated autophagy
494 modulator DRAM1 links mycobacterial recognition via TLP-MYD88 to authophagic
495 defense. Cell Host Microbe 15:753–767.
496 36. Stoop EJ, Schipper T, Huber SK, Nezhinsky AE, Verbeek FJ, Gurcha SS, Besra GS,
497 Vandenbroucke-Grauls CM, Bitter W, van der Sar AM. 2011. Zebrafish embryo screen
498 for mycobacterial genes involved in the initiation of granuloma formation reveals a
499 newly identified ESX-1 component. Dis Model Mech2011/03/05. 4:526–536.
500 37. van der Vaart M, van Soest JJ, Spaink HP, Meijer AH. 2013. Functional analysis of a
501 zebrafish myd88 mutant identifies key transcriptional components of the innate
502 immune system. Dis Model Mech 6:841–854.
503 38. Ogryzko N V., Hoggett EE, Solaymani-Kohal S, Tazzyman S, Chico TJA, Renshaw SA,
504 Wilson HL. 2014. Zebrafish tissue injury causes upregulation of interleukin-1 and
505 caspase-dependent amplification of the inflammatory response. Dis Model Mech
506 7:259–264.
507 39. Benard EL, Rougeot J, Racz PI, Spaink HP, Meijer AH. 2016. Transcriptomic
508 Approaches in the Zebrafish Model for Tuberculosis—Insights Into Host- and
509 Pathogen-specific Determinants of the Innate Immune Response. Adv Genet 95:217–
510 251.
511 40. Cohen P. 2014. The TLR and IL-1 signalling network at a glance. J Cell Sci 127:2383–
512 2390.

513 41. Ogryzko N V., Renshaw SA, Wilson HL. 2014. The IL-1 family in fish: Swimming
514 through the muddy waters of inflammasome evolution. Dev Comp Immunol.
515 42. Hasegawa T, Hall CJ, Crosier PS, Abe G, Kawakami K, Kudo A, Kawakami A. 2017.
516 Transient inflammatory response mediated by interleukin-1β is required for proper
517 regeneration in zebrafish fin fold. Elife 6.
518 43. Kanther M, Sun X, Mhlbauer M, MacKey LC, Flynn EJ, Bagnat M, Jobin C, Rawls JF.
519 2011. Microbial colonization induces dynamic temporal and spatial patterns of NF-
520 ??B activation in the zebrafish digestive tract. Gastroenterology 141:197–207.
521 44. Ulrichs T, Kaufmann SH. 2006. New insights into the function of granulomas in human
522 tuberculosis. J Pathol2005/12/20. 208:261–269.
523 45. Flynn JL, Chan J, Lin PL. 2011. Macrophages and control of granulomatous
524 inflammation in tuberculosis. Mucosal Immunol2011/03/25. 4:271–278.
525 46. Via LE, Lin PL, Ray SM, Carrillo J, Allen SS, Eum SY, Taylor K, Klein E, Manjunatha U,
526 Gonzales J, Lee EG, Park SK, Raleigh JA, Cho SN, McMurray DN, Flynn JL, Barry 3rd CE.
527 2008. Tuberculous granulomas are hypoxic in guinea pigs, rabbits, and nonhuman
528 primates. Infect Immun2008/03/19. 76:2333–2340.
529 47. Orphanidou D, Gaga M, Rasidakis A, Dimakou K, Toumbis M, Latsi P, Pandalos J,
530 Christacopoulou J, Jordanoglou J. 1996. Tumour necrosis factor, interleukin-1 and
531 adenosine deaminase in tuberculous pleural effusion. Respir Med 90:95–98.
532 48. Waitt CJ, Banda P, Glennie S, Kampmann B, Squire SB, Pirmohamed M, Heyderman
533 RS. 2015. Monocyte unresponsiveness and impaired IL1β, TNFα and IL7 production
534 are associated with a poor outcome in Malawian adults with pulmonary tuberculosis.
535 BMC Infect Dis 15:513.
536 49. Robinson CM, Nau GJ. 2008. Interleukin-12 and interleukin-27 regulate macrophage

control of Mycobacterium tuberculosis. J Infect Dis 198:359–366.

50. Zhang W, Petrovic JM, Callaghan D, Jones A, Cui H, Howlett C, Stanimirovic D. 2006. Evidence that hypoxia-inducible factor-1 (HIF-1) mediates transcriptional activation of interleukin-1?? (IL-1??) in astrocyte cultures. J Neuroimmunol 174:63–73.

51. Charbonneau M, Harper K, Grondin F, Pelmus M, McDonald PP, Dubois CM. 2007. Hypoxia-inducible factor mediates hypoxic and tumor necrosis factor alpha-induced increases in tumor necrosis factor-alpha converting enzyme/ADAM17 expression by synovial cells. J Biol Chem 282:33714–24.

52. Malik A, Kanneganti T-D. 2017. Inflammasome activation and assembly at a glance. J Cell Sci 130:3955–3963.

Figure Legends

Figure 1. Dominant active Hif-1α mediated increase in anti-nitrotyrosine signal is Myd-88 independent.

(A) Cartoon of embryo showing position of imaging for panels in A. Example fluorescence confocal z-stacks of the caudal vein region of embryos stained with Alexa-633 labeled anti-nitrotyrosine antibody (red), imaged at 1dpi in the presence or absence of Mm infection. One-cell stage embryos were injected with phenol red (PR) or dominant active Hif-1α (DA1). One-cell stage embryos we co-injected with *myd88* morpholino or (myd88 MO) or standard control morpholino (Cont MO). At 1dpi larvae were either infected with Mm mCherry (Mm), or PVP as a non-infected control (Mm channel not shown in these panels).

(B) Corrected fluorescence intensity levels of anti-nitrotyrosine antibody confocal z-stacks of phenol red (PR) control injected embryos in the presence or absence of

Mm infection at 1dpi. Control morpholino is shown in the clear bars and *myd88* morpholino (myd-88 MO) in the filled bars. Data shown are mean ± SEM, n=70-72 cells from 10-12 embryos accumulated from 3 independent experiments.

Figure 2. *TgBAC(il-1β:GFP)sh445* is activated upon tailfin injury in first neutrophils, then macrophages.

(A) Wholemount *in situ* hybridisation of *il-1β* in tailfin injured 2dpf embryos.

(B) Fluorescent confocal micrographs of *TgBAC(il-1β:GFP)sh445* expression after tailfin injury. Upper and lower panels show the same individual embryo 0 and 12hpi.

(C) Cartoon of embryo showing position of imaging area of D and E and the dotted line of tailfin transection.

(D) Fluorescent confocal micrographs of *TgBAC(il-1β:GFP)sh445* crossed to *Tg(lyz:Ds- RED2)nz50* labeling neutrophils at 1 hour post wound (1hpw) and 6hpw.

(E) Fluorescent confocal micrographs of *TgBAC(il-1β:GFP)sh445* crossed to *Tg(mpeg1:mCherryCAAX)sh378* line labeling macrophages at 1 hour post wound (1hpw) and 6hpw.

Figure 3. *il-1β:GFP* is upregulated by Mm in infected macrophages at early and later stage infection

A) Graph showing relative *il-1β* mRNA expression by SYBERgreen qPCR in Mm infected 1dpi larvae (Mm) and mock injected controls (PVP). Data shown are mean ± SEM, n=3 independent experiments.

(B) Fluorescent confocal micrographs of 1dpi, prior to granuloma formation (left panel), and at 4dpi, in immune cells in blood vessels (middle panel, blood vessel indicated by solid white lines) and early tissue granuloma (right panel). *il-1β*

expression was detected by GFP levels, in green, using the *TgBAC(il-1:eGFP)sh445* transgenic line. Mm mCherry is shown in the red channel. Increased levels of *il-1β:GFP* expression were detectable in cells associated with infection.

(C) Fluorescent confocal micrographs of a timelapse between 6 to 8 hours post Mm infection. Mm mCherry is shown in the red channel and *il-1β:GFP* in the green channel with the microscope settings set to detect low GFP levels. Arrowheads indicate the emergence of *il-1β:GFP* expression in an infected cell.

(D) Cartoon of embryo showing position of imaging for panels in D. Fluorescent confocal micrographs of 1dpi caudal vein region of infection. *il-1β* expression was detected by GFP levels, in green, using the *TgBAC(il-1β:eGFP)sh445* transgenic line. Macrophages are shown in red using a *Tg(mpeg1:mCherryCAAX)sh378* line. Mm Crimson is shown in the blue channel (right panels) with a PVP control (left panels). Without infection there is little overlap of *il-1β:GFP* and *mpeg:mCherry*, while in infected larvae macrophages have higher levels of *il-1β:GFP*. Arrowheads indicate infected macrophages with high levels of *il-1β:GFP.* Dotted lines indicate the yolk extension of the larvae where there is non-specific fluorescence.

Figure 4. *il-1β:GFP* is upregulated in the absence of infection by DA Hif-1α

(A) Cartoon of embryo showing position of imaging for panels in A. Fluorescent confocal micrographs of 1dpi caudal vein region of infection. *il-1β:GFP* expression was detected by GFP levels, in green, using the *TgBAC(il-1:eGFP)sh445* transgenic line. Larvae were injected at the 1 cell stage with dominant negative (DN) or dominant active (DA) Hif-1α or phenol red (PR) control. Non-infected larvae are in the left panels (PVP) and Mm Crimson infected larvae are in the right panels (Mm).

Dotted lines indicate the yolk extension of the larvae where there is non-specific fluorescence.

(B) Corrected fluorescence intensity levels of *il-1β:GFP* confocal z-stacks in uninfected larvae (PVP, empty bars) and infected larvae (Mm, filled bars) at 1dpi. Dominant active Hif-1α (DA1) had significantly increased *il-1β:GFP* levels in the absence of Mm bacterial challenge compared to phenol red (PR) and dominant negative Hif-1α (DN1) injected controls. Data shown are mean ± SEM, n=24-48 cells from 4-8 embryos representative of 3 independent experiments.

Figure 5. *il-1β* knockdown abrogated the protective effect of DA Hif-1α on bacterial burden and anti-nitrotyrosine production

(A) Bacterial burden at 4dpi after injection of DA Hif-1α (DA1) and the *il-1β* morpholino (Il-1 MO), using the standard control morpholino and phenol red (Control) as a negative control. Data shown are mean ± SEM, n=46-50 as accumulated from 3 independent experiments.

(B) Bacterial burden of *il-1β* (il-1-/-) and sibling wildtype controls (WT) at 4dpi after injection of DA Hif-1α (DA1) or phenol red (PR) as a negative control. Data shown are mean ± SEM, n=16-20 as accumulated from 3 independent experiments.

(C) Cartoon of embryo showing position of imaging for panels in C. Example fluorescence confocal z-stacks of the caudal vein region of embryos stained with Alexa-633 labeled anti-nitrotyrosine antibody (red), imaged at 1dpi in the presence or absence of Mm infection. One-cell stage embryos were injected with phenol red (PR, left panel) or dominant active Hif-1α (DA1, right panel). One-cell stage embryos we co-injected with *il-1β* morpholino or (il-1 MO) or standard control morpholino (Cont

MO). At 1dpi larvae were either infected with Mm mCherry (Mm), or PVP as a non-infected control (Mm channel not shown in these panels).

(D) Corrected fluorescence intensity levels of anti-nitrotyrosine antibody confocal z-stacks of phenol red (PR) control injected embryos in the presence or absence of Mm infection at 1dpi. Control morpholino is shown in the clear bars and *il-1β* morpholino (il-1 MO) in the filled bars. Data shown are mean ± SEM, n=54-59 cells from 10-12 embryos accumulated from 3 independent experiments.

(E) Corrected fluorescence intensity levels of anti-nitrotyrosine antibody confocal z-stacks of dominant active Hif-1α (DA1) injected embryos in the presence or absence of Mm infection at 1dpi. Control morpholino is shown in the clear bars and il-1 morpholino (il-1 MO) in the filled bars. Data shown are mean ± SEM, n=54-59 cells from 10-12 embryos accumulated from 3 independent experiments.

Supplemental Figure 1. CRISPR-Cas9 *il-1β SH446* mutant.

(A) Screenshot of Ensembl zebrafish *il-1β* coding sequence with CRISPR-Cas9 target indicated in the fourth exon.

(B) DNA alignment of WT *il-1β* sequence and *il-1βSH446* showing the 44 base pair deletion caused by CRISPR-Cas9.

(C) Amino acid alignment of WT *il-1β* sequence and *il-1βSH446* with arrowhead showing the premature stop and removal of the putative Il-1β cleavage site.

(D) Sequencing trace showing position of CRISPR-Cas9 induced deletion.

Supplemental Movie 1. *Il-1β:GFP* expression in activated immune cells after Mm infection.

(A) Fluorescent confocal videotimelapse of *il-1β:GFP* in immune cells containing Mm infection (*il-1β:GFP* in green and Mm mCrimson in red).

Figure 1

A

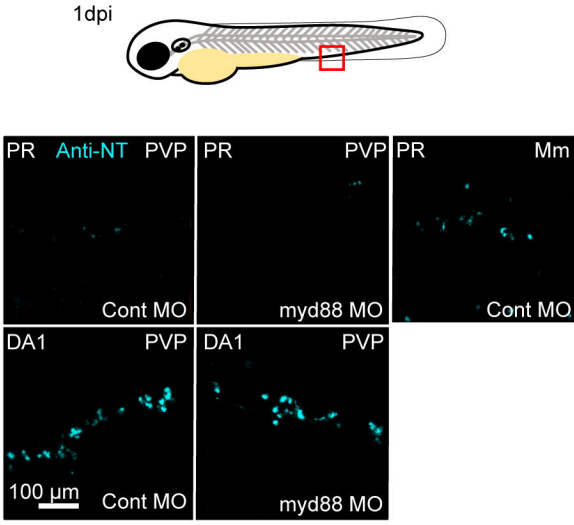
1dpi
PR
Anti-NT
PVP
Cont MO
PR
PVP
myd88 MO
PR
Mm
Cont MO
DA1
PVP
100 µm
Cont MO
DA1
PVP
myd88 MO

B

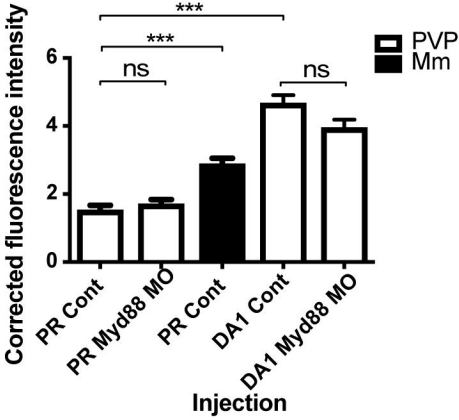
***
***
ns
ns
PVP
Mm
Corrected fluorescence intensity
0
2
4
6
PR Cont
PR Myd88 MO
PR Cont
DA1 Cont
DA1 Myd88 MO
Injection

Figure 2

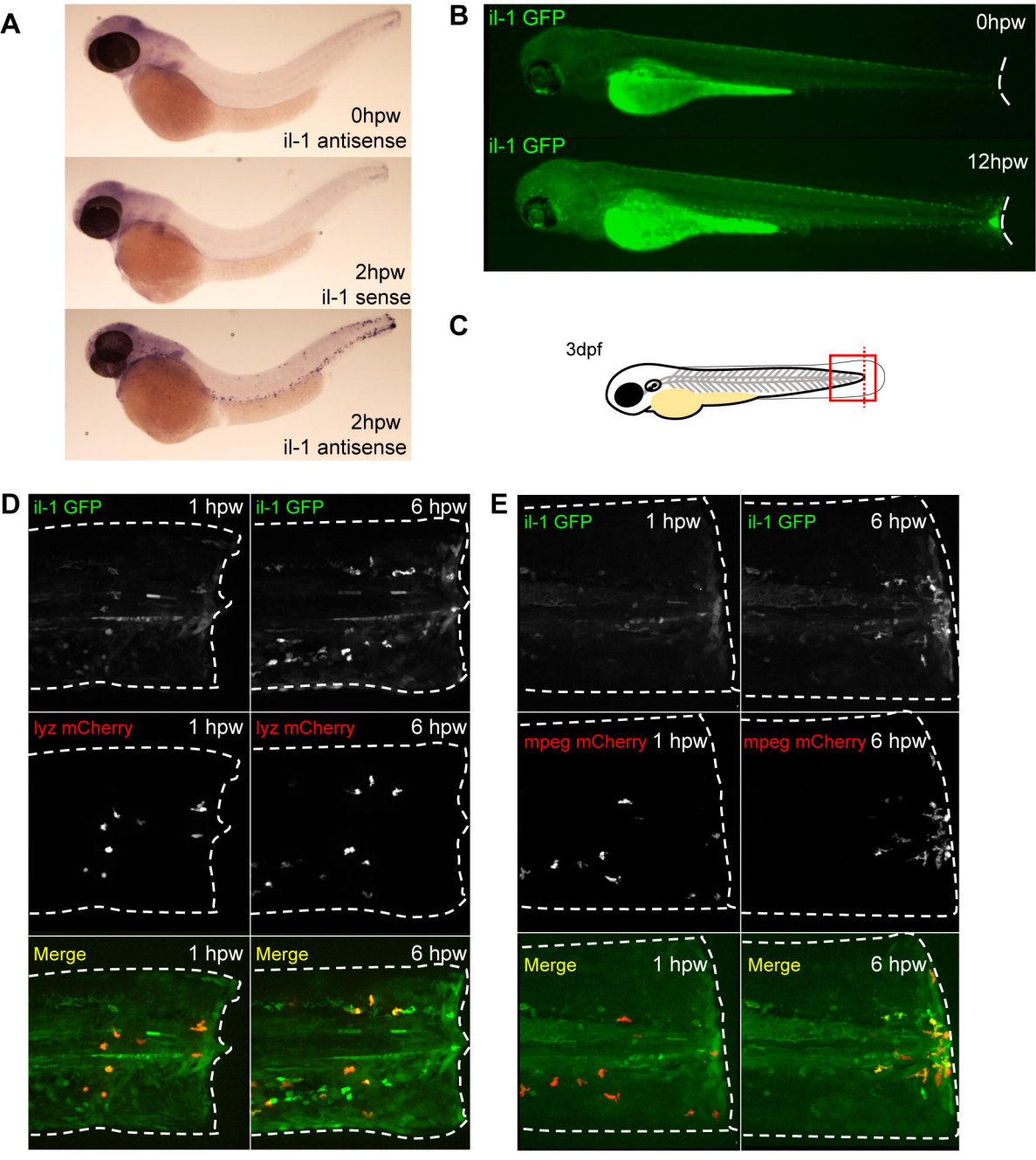
A
0hpw
il-1 antisense
2hpw
il-1 sense
2hpw
il-1 antisense
B
il-1 GFP
0hpw
il-1 GFP
12hpw
C
3dpf
D
il-1 GFP
1 hpw
il-1 GFP
6 hpw
lyz mCherry
1 hpw
lyz mCherry
6 hpw
Merge
1 hpw
Merge
6 hpw
E
il-1 GFP
1 hpw
il-1 GFP
6 hpw
mpeg mCherry
1 hpw
mpeg mCherry
6 hpw
Merge
1 hpw
Merge
6 hpw

Figure 3

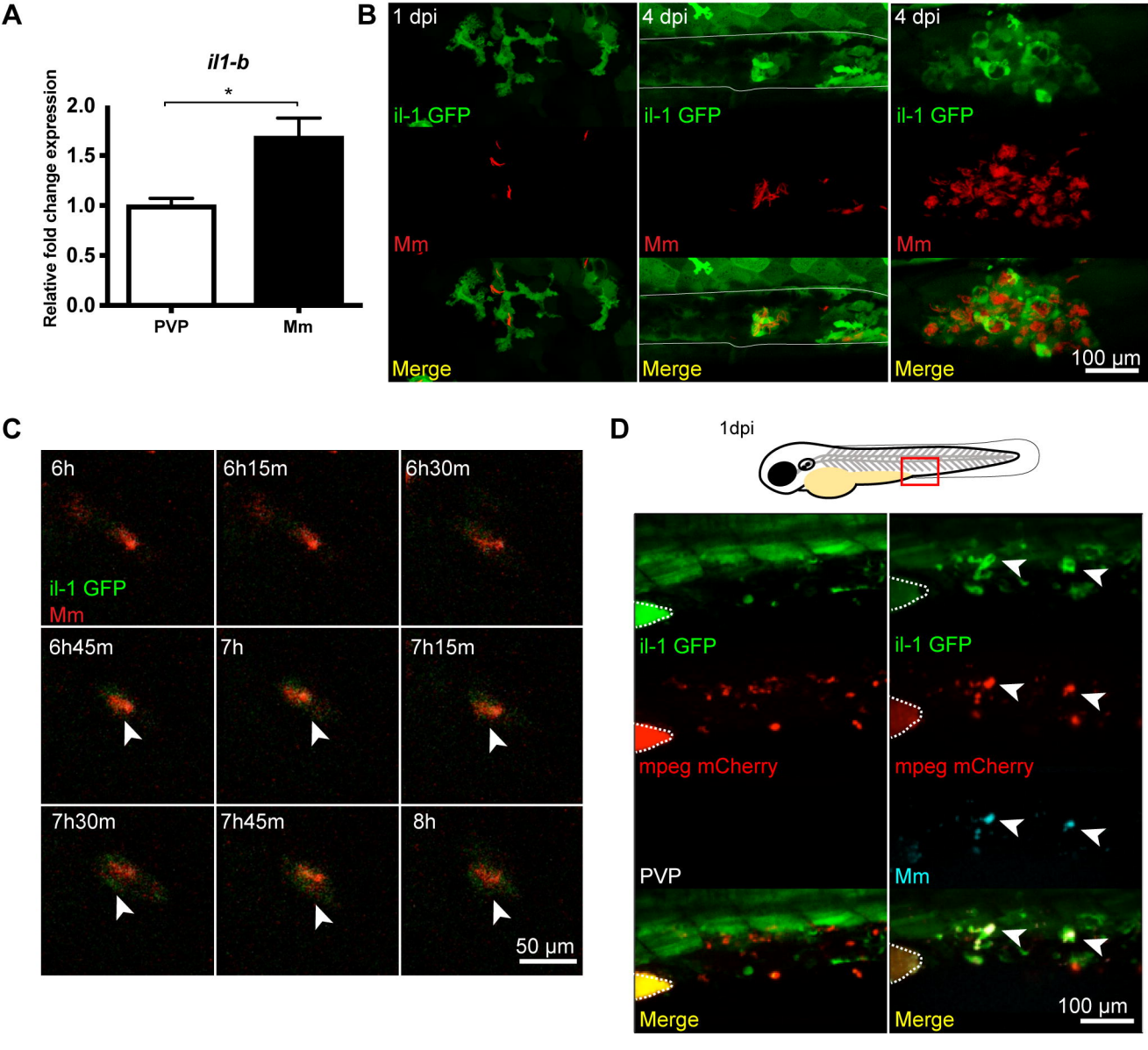
A
il1-b
*
Relative fold change expression
2.0
1.5
1.0
0.5
0.0
PVP
Mm
B
1 dpi
4 dpi
4 dpi
il-1 GFP
Mm
Merge
100 µm
C
6h
6h15m
6h30m
6h45m
7h
7h15m
7h30m
7h45m
8h
il-1 GFP
Mm
50 µm
D
1dpi
il-1 GFP
mpeg mCherry
PVP
Mm
Merge
100 µm

Figure 4

A

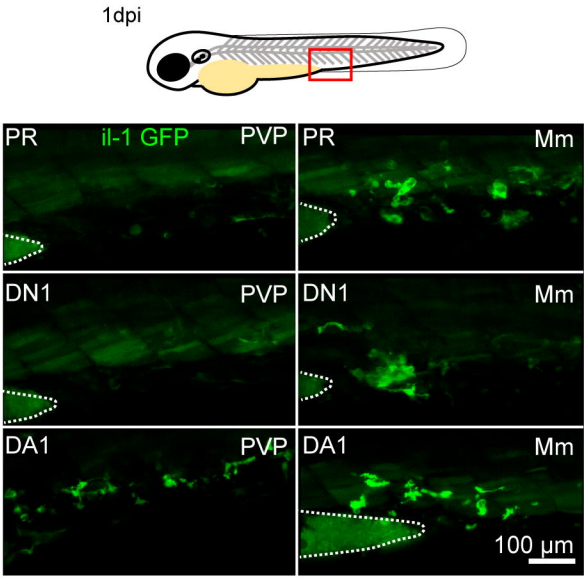
1dpi
PR
il-1 GFP
PVP
PR
Mm
DN1
PVP
DN1
Mm
DA1
PVP
DA1
Mm
100 µm

B

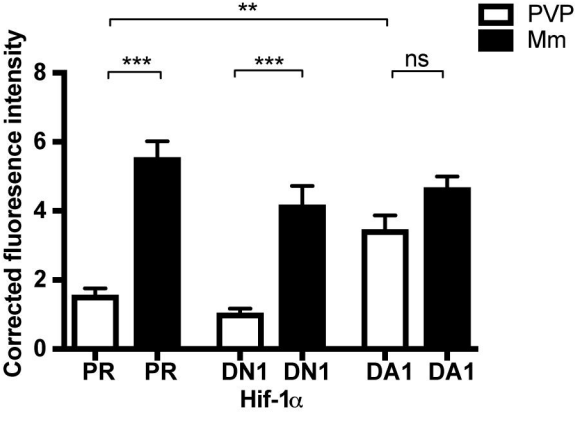
**
***
***
ns
PVP
Mm
Corrected fluoresence intensity
0
2
4
6
8
PR
PR
DN1
DN1
DA1
DA1
Hif-1α

Figure 5

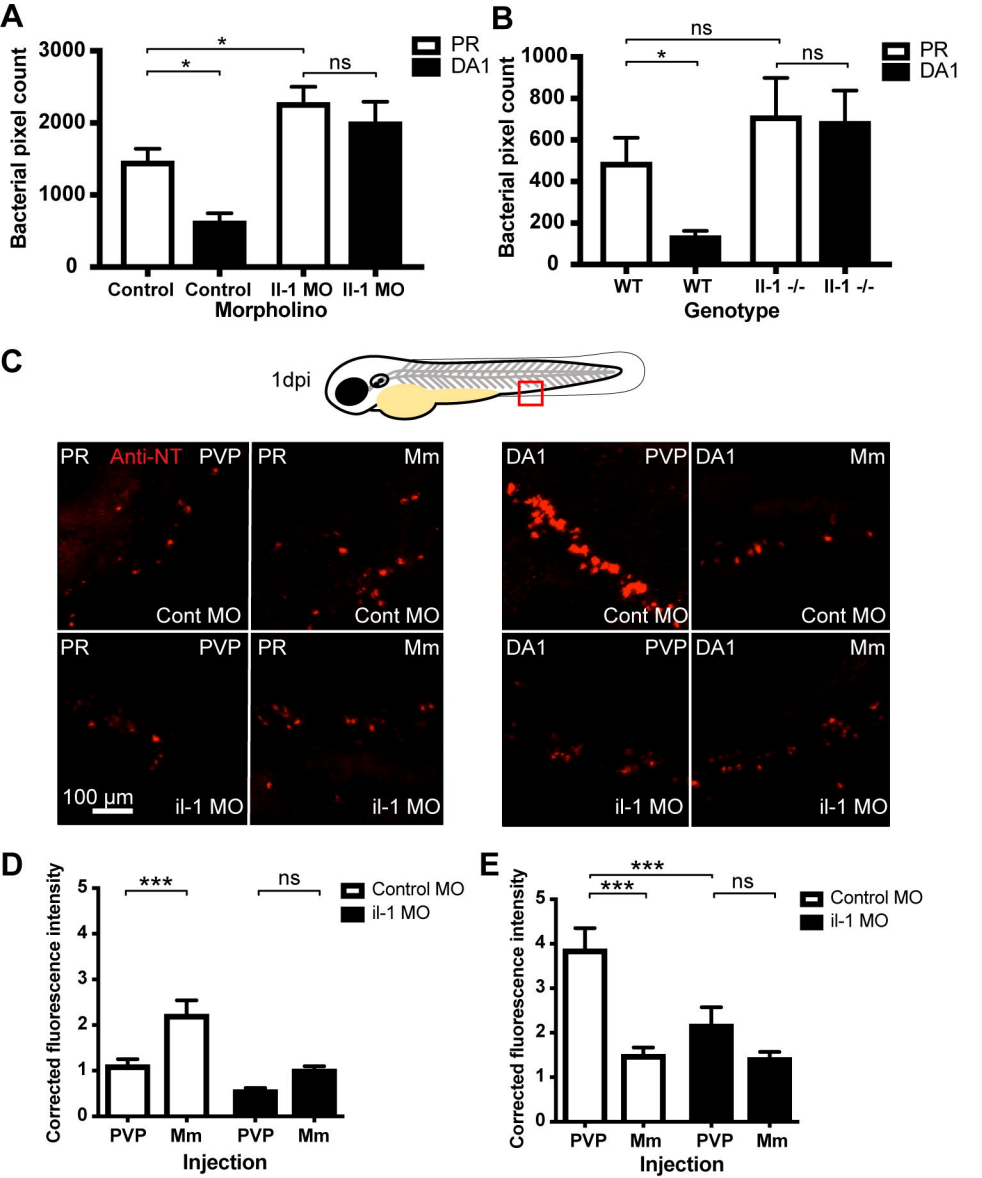
A
Bacterial pixel count
3000
2000
1000
0
*
*
ns
PR
DA1
Control
Control
Il-1 MO
Il-1 MO
Morpholino
B
Bacterial pixel count
1000
800
600
400
200
0
ns
*
ns
PR
DA1
WT
WT
Il-1 -/-
Il-1 -/-
Genotype
C
1dpi
PR
Anti-NT
PVP
Cont MO
PR
Mm
Cont MO
DA1
PVP
Cont MO
DA1
Mm
Cont MO
PR
PVP
il-1 MO
PR
Mm
il-1 MO
DA1
PVP
il-1 MO
DA1
Mm
il-1 MO
100 µm
D
Corrected fluorescence intensity
5
4
3
2
1
0
***
ns
Control MO
il-1 MO
PVP
Mm
PVP
Mm
Injection
E
Corrected fluorescence intensity
5
4
3
2
1
0
***
***
ns
Control MO
il-1 MO
PVP
Mm
PVP
Mm
Injection